Also publisehd as ACI SP-326—58

Next generation UHPFRC for sustainable structural applications

Amir Hajiesmaeili and Emmanuel Denarié

Synopsis: Over the last few decades, ever-increasing demands of society to the built environment have continually increased consumption of energy and materials for the construction and maintenance of structures. Meanwhile, Strain Hardening Ultra High-Performance Fiber Reinforced Concrete (SH-UHPFRC) have the potential to be one of the solutions to contain the explosion of maintenance costs (Economy and Environment), considering their extremely low permeability associated to outstanding mechanical properties and load bearing efficiency compared to deadweight.

The objective of this research is to further improve the already established concept of UHPFRC application for rehabilitation. This paper reports firstly on the development and validation of new low Embodied Energy (EE) SH-UHPFRC mixes with 50 % clinker replacement by Supplementary Cementitious Materials and replacement of steel fibers by ultra-high molecular weight polyethylene (UHMW-PE) ones. In a second step, the mechanical and protective properties of the mixes are investigated with a special emphasis on their quasi-static tensile response, and transport properties. Finally, the dramatic improvement in terms of reduction of EE and deadweight of the proposed mixes is demonstrated.

Keywords: UHPFRC; Strain Hardening; Packing density; Embodied Energy; Water sorptivity; UHMW PE fibers; Durability

Biography: **Amir Hajiesmaeili** is a Ph.D. student at Division of Maintenance and Safety of Structures (MCS-IIC-ENAC), Ecole Polytechnique Fédérale de Lausanne (EPFL) He received his BS and MS from University of Tehran. His research interests include UHPFRC and its structural applications.

ACI member **Emmanuel Denarié,** a civil engineer, dr. ès sciences techniques, is senior scientist in the Division of Maintenance and Safety of structures (MCS-IIC-ENAC), at Ecole Polytechnique Fédérale de Lausanne (EPFL). He has 30 years' experience in research, development and applications in the field of advanced cementitious materials. He is involved in various research programs related to the development of UHPFRC and is also a lecturer at the EPFL.

INTRODUCTION

Over the last few decades, ever-increasing demands of society to the built environment have continually increased consumption of energy and materials for the construction of new structures and for the maintenance of existing ones. Meanwhile, Strain Hardening Ultra High-Performance Fiber Reinforced Concrete (SH-UHPFRC) have the potential to be one of the solutions to contain the explosion of maintenance costs (Economy and Environment), considering their extremely low permeability associated to outstanding mechanical properties and load bearing efficiency compared to deadweight.

Currently, UHPFRC is gaining ground in the field of rehabilitation of the structures and it is frequently used for new construction applications. Habert et al. [1] showed that using UHPFRC based system for rehabilitation can reduce the environmental impact by a factor two compared to the conventional concrete solution considering the service life. Among the applications with UHPFRC, there are only a few notable ones, which have been conducted using synthetic fibers and the rest are almost exclusively based on steel fibers. The synthetic fibers are mostly used in UHPFRC for facade elements with complex shapes [2]. Considering the fact that more than 50% of the EE and Global Warming Potential (GWP) impact of the UHPFRC is from the steel fibers contribution [3], replacing the steel fibers with synthetic ones for structural applications would have a very positive effect on reducing the environmental costs of this material.

The first attempts in order to achieve a strain-hardening cementitious composites with synthetic fibers have started from the 1990s. Li [4] used micromechanics theory in order to obtain strain hardening cementitious material reinforced with PE or PVA fibers. ECC (Engineered Cementitious Composite) was the result of his research; a material with evenly distributed multiple microcracks, around 4.5 MPa tensile strength, 40 MPa compressive strength, and 5% strain hardening capacity. This trend has been continued by introducing Strain Hardening Cementitious Composites (SHCC) and UHP-SHCC. Kunieda et al. [5] and Kamal [6] achieved a cementitious material with significant strain hardening capacity (close to 1%), relatively high compressive strength (83 MPa), and tensile strength of 4.5 MPa using high-performance PE fibers. A more recent development is the use of UHMW PE fibers in High-Strength, High-Ductility Concrete (HSHDC) [7]. The authors achieved an ultimate tensile strength of 14 MPa at 3.5% deformation and compressive strength of 160 MPa. Most recently, Curosu et al. [8] investigated the tensile behavior of high-strength strain-hardening cement-based composites (HS-SHCC) using high-density polyethylene (HDPE) and achieved 7.6 MPa ultimate tensile strength at 14 days and 133.5 MPa compressive strength.

The objective of this research is to further improve the already established concept of UHPFRC mixes with steel fibers applied for rehabilitation. This paper reports firstly on the development and validation of new low EE SH-UHPFRC mixes with 50 % clinker replacement by Supplementary Cementitious Materials and replacement of steel fibers by ultra-high molecular weight polyethylene (UHMW-PE) ones. In a second step, the mechanical and protective properties of the mixes are investigated with a special emphasis on their quasi-static tensile response, and transport properties. Finally, the dramatic improvement in terms of reduction of Embodied Energy and deadweight of the proposed mixes is highlighted.

MATERIAL DESIGN

Key concepts for designing a cementitious material are the packing density and the workability. The packing characteristics of the cementitious materials greatly influence both the mechanical and durability properties of the mix as well as its water demand at fresh state. Beginning as early as the 1960s, Powers [9] suggested to consider the concrete mixture as a solid skeleton and voids, which have to be filled with water at fresh state. Therefore, reducing the voids in the solid grains skeleton frees batching water to lubricate the solid particles and enhance the workability [10]. Hence, increasing packing can improve the overall workability-strength performance of the cementitious material by opening up the possibility of using very low W/B ratios.

In 1999, de Larrard [11] introduced the Compressible Packing Model (CPM) in order to model and maximize the packing density of cementitious materials. This model considers the energy required to compact a mix of several monosized particle classes. It also considers the loosening effect on large particles by interstitial small ones, and the wall effect within assemblies of small particles near a large one, as well as fibers or a container wall. Sedran [12] generalized the CPM to consider the interaction of multiple grain classes with arbitrary Particle Size Distributions (PSD). Focusing on the interaction equations for the particles smaller than 125 μm, Fennis, Walraven [13] developed the Compaction-Interaction Packing Model (CIPM) which is an extension of the CPM, taking due account of surface forces like van der Waals forces, electrical double layer forces and steric forces.

In this study, the generalized CIPM model is developed and used, in order to consider the interaction of grain classes with arbitrary PSD as well as the interaction equations for the particles smaller than 125 μm which are necessary for UHPFRCs. Five different powders including cement, two types of limestone filler, silica fume and sand were used in the mixes.

Model development

The CPM model [11], predicts the packing density of the mix containing *n* monosized classes by considering the geometrical parameters (loosening and wall effects) and energy of the mixing. In order to implement more realistically the variance in compaction energy of the different granular fractions in the CIPM, Fennis et al. [13] used Eq. 1 which is, originally proposed by de Larrard [11]. The actual packing density (Φ) is obtaining by solving the Eq. 1 for Φ.

$$K = \sum_{i=1}^{n} \frac{\varphi_i / \varphi_i^*}{1 - \varphi_i / \varphi_i^*} \tag{1}$$

Where φ_i/φ_i^* is written as Eq. 2.

$$\frac{\varphi_i}{\varphi_i^*} = \frac{r_i \Phi}{\beta_i \left(1 - \sum_{j=1}^{i-1} [1 - b_{ij}(1 - 1/\beta_j)] r_j \Phi - \sum_{j=i+1}^{n} [a_{ij} \beta_i / \beta_j] r_j \Phi \right)} \tag{2}$$

Where,

K = Compaction index depends on the compaction energy applied to the mixture.

r_i = Volume fraction of size class i

β_i = virtual packing density of size class i (Eq. 3)

$$\beta_i = \alpha_i \left(1 + \frac{1}{K}\right) \tag{3}$$

Where,

α_i = Experimentally determined packing density of class i for a prescribed packing process and K value

Table 1 presents K values for various packing processes.

The geometrical interaction between size classes is represented by a_{ij} for the loosening effect and b_{ij} for the wall effect as is shown in Eq. 4 and Eq. 5 respectively. In order to consider the interaction of the particles smaller than 125 μm, Fennis et al. [13] modified the de Larrard's [11] interaction functions on the basis of the works of Schwanda [14].

$$a_{ij} = \begin{cases} 1 - \dfrac{\log_{10}(d_i/d_j)}{w_{0,a}} & \log_{10}(d_i/d_j) < w_{0,a} \\ 0 & \log_{10}(d_i/d_j) \geq w_{0,a} \end{cases}, \quad w_{0,a} = \begin{cases} w_a \times C_a & d_j < d_c \\ w_a & d_j \geq d_c \end{cases} \tag{4}$$

$$b_{ij} = \begin{cases} 1 - \dfrac{\log_{10}(d_j/d_i)}{w_{0,b}} & \log_{10}(d_j/d_i) < w_{0,b} \\ 0 & \log_{10}(d_j/d_i) \geq w_{0,b} \end{cases}, \quad w_{0,b} = \begin{cases} w_b \times C_b & d_i < d_c \\ w_b & d_i \geq d_c \end{cases} \tag{5}$$

In which,

d_i and d_j are the diameter of size class i and class j, respectively.

d_c is the transition diameter in the CIPM below which compaction-interaction is taken into account.

$w_{0,a}$ and $w_{0,b}$ are the functions for maximum range of loosening effect and wall effect respectively.

w_a and w_b are the constants denoting the maximum range of loosening effect and wall effect respectively.

C_a and C_b are the compaction-interaction constant within the loosening effect and wall effect respectively.

However, in reality, the components which are used in UHPFRC have a wide range of particle sizes and they are not monosized without interaction. In order to consider this, Eq. 1 is generalized as Eq. 6 considering *M* different material and *n* different size classes [15]

$$K = \sum_{i=1}^{n} \frac{\sum_{k=1}^{M} \frac{\varphi_{k,i}}{\beta_{k,i}}}{\sum_{k=1}^{M} \varphi^{*}_{k,i} / \beta_{k,i} - \sum_{k=1}^{M} \varphi_{k,i} / \beta_{k,i}} \quad (6)$$

Where,

$$\varphi_{k,i} = p_k \cdot r_{k,i} \cdot \Phi \quad (7)$$

$$\varphi^{*}_{k,i} = \beta_{k,i}\, \mathrm{p}_k \left[1 - \left[\sum_{j=1}^{i-1} [1 - b_{ij}(1 - 1/\beta_{k,j})] r_{k,j} \Phi + \sum_{j=i+1}^{n} a_{ij} r_{k,j} \Phi / \beta_{k,j} \right] \right] \quad (8)$$

In which
p_k = Volume fraction of material *k*
$r_{k,i}$ = Volume fraction of material *k* in class *i*
$\beta_{k,i}$ = virtual packing density of material *k* in class *i*

Packing density of the components

Although a number of theoretical packing models have been developed and applied, accurate measurement of the packing density of very fine materials, such as the cementitious materials used in concrete, has remained a difficult task. BS812 [16] has specified a dry packing method for measuring the bulk density of aggregate. However, due to the adhesion phenomena from Van der Waals and electrostatic forces between the particles this method is not proper for the powders smaller than 100 μm.

In this study, in order to measure the packing density of the fine powder more accurately, the water demand method based on mixing energy [17] has been used. The water demand of the mix is determined as the water addition (combined to superplasticizer) at which maximum mixing power is measured. the packing density of the sand was measured using dry packing method [16].

EXPERIMENTAL PROGRAM

The experimental program was designed in a way to investigate and compare both the mechanical and durability properties of the mixes. Two UHPFRC mixture with and without fine sand, with different packing densities were designed. In these mixes, 50% volume of clinker is replaced by two types of limestone filler.

Five different powders including cement CEM I 52.5 HTS Lafarge, two types of limestone filler (Betoflow D® and Betocarb SL® from OMYA), white silica fume from SEPR (BET = 14 m^2/gr), and sand from SIBELCO type BE01, SP type SIKA Viscocrete P5 and UHMW PE fibers form DYNEEMA type SK99 were used in the mixtures..

The generalized CIPM model has been used for the packing density calculations. After Fennis (2001), cementitious material with superplasticizer can be modeled with $w_a = w_b = 1$, $C_a = 1.5$, $C_b = 0.2$ and $d_c = 25$ μm. Furthermore, the particle size distribution of the components and of the two mixes are shown in **Figure 1**.

The mixture proportions of the two UHPFRC with reduced cement amount are given in **Table 2** together with, for reference, Mix (III) (Ductal® NaG3 TX SH-UHPFRC mix with steel fibers), which was used in rehabilitation of chillon viaducts [18] and is frequently used on the Swiss market. The packing density of the mixes is calculated and presented in the same table.

After casting, all specimens were sealed with a plastic cover and stored after demolding at room temperature of 20 ± 5°C under 95 % RH, before testing at 14 days for mechanical tests and 28 days for capillary absorption.

Mechanical properties

Direct tensile tests were performed under quasi-static uniaxial loading under displacement control with a stroke rate of 0.4 mm/min. **Figure 2** shows the dumbbell specimens geometry based on JSCE [19] recommendation which were used in this study. The specimens were gripped on their faces in a fixed-fixed type of end constraints using a wedge-clamping system. The gauge length of the 2 LVDTs was 150 mm.

4-point bending tests on 100x500x30 mm plates were done following Denarié et al. [18]. The tests were performed under displacement control at a stroke rate of 0.5 mm/min. The span was 420 mm and the loading span was 140 mm. The force was measured by the load cell of the testing machine, and the mid-span deflection was recorded using two LVDTs placed at mid-span, attached to a measuring frame fixed to the middle axis of the specimen, on the support points, during the test.

The compressive strength of the mixes was investigated by using 70x140 mm cylinders according to SIA 2052:2016 [20].

Durability properties

The capillary absorption test was chosen in order to investigate the durability properties. This test was conducted in accordance with standard EN13057:2002 [21]. For each mixture, two plates of 200x500x30 mm were cast. First, 100 mm cores were cut from the plates, the cores were dried at 50° C up to a constant weight, then stored in the laboratory atmosphere for at least 12 hours. Afterward, the lateral surface of the cores was coated with an epoxy resin so that only one circular face of the specimen was exposed to water. The water level during the test was kept constant and 2 mm above the surface of the specimen in contact with water. The weight of specimens was monitored over a period of time (0–144 h) along the contact with water. Throughout the test, temperature and humidity were kept constantly at 20-22° C and 95%, respectively.

RESULTS AND DISCUSSION

Mechanical properties

The direct tensile response of the mixes (I) and (II) together with that of the M-HDPE mix from Curosu et al. [8] are presented in **Figure 3** and **Figure 4**, respectively. The results are presented in the stress-strain format. The x-axis in these figures shows the average tensile strain computed from the extensions of two LVDTs. The M-HDPE mix contains 1460 kg/m^3 (91.1 lb/ft^3) cement, 292 kg/m^3 (18.2 lb/ft^3) silica fume and 145 kg/m^3 (9.0 lb/ft^3) fine quartz sand. As the results show, all the specimens exhibited tensile strain-hardening behavior. Although in the mix (I) and (II) more than 50% of clinker is replaced with limestone filler compared with M-HDPE from Curosu et al. [8], the ultimate strength and deformability of the two mixes are in a similar range of 9 MPa and 4%, respectively. However, a difference in the behavior of the two mixes can be noticed in the elastic limit. Mix (II), with a highe value of packing density due to the beneficial effect of the coarser fine sand grains, shows a higher elastic limit.

The 4-point bending force-deflection response of the mixes is shown in **Figure 5**. The results follow the same trend as that of the direct tensile tests. The ultimate forces are in a similar range for both mixes, although the deformability of mix (I) is more than mix (II). Furthermore, as it is shown in **Figure 6**, the deviation from linearity is also following the same trend as the direct tensile test, that is, the results of the mix with lower packing density, deviate earlier from linearity. Comparing the maximum forces of mixes (I) and (II) with that of mix (III), shows that both of the new mixes are in the same range typical of SH-UHPFRC with steel fibers despite replacing 50% of clinker by limestone filler and 100% of steel fibers by UHMW PE fibers.

Table 3, presents the compressive strength of two new UHPFRC mixes and Mix (III). The compression test was done on 70x140mm cylinders for Mix (II) and Mix (III) and the results of the compression test on 40x40x160 mm prisms for Mix I were scaled to be comparable with 70x140mm cylinder results according to SIA 2052 [20]. The compressive strength of mix (II) shows 40% higher value compared to the results of mix (I) which confirms the better quality of its matrix. Moreover, the compressive strength of mix (II) is in the same range as the results of reference mix (III).

Durability properties

The capillary absorption results of the investigated mixes are presented in **Table 4**. The sorption coefficient, *S*, is obtained from the slope of the cumulative mass of water absorbed per unit of area of inflow surface versus square root of time, calculated for 24 h per [21], as represented in Eq. 13.

$$S = \frac{m_w}{A\sqrt{t}} \tag{13}$$

Where,

m_w is the mass of water absorbed by the specimen (gr)

A is the cross-sectional area of each specimen (m^2) and

t is the time of exposure (h).

According to the test results, as expected, the capillary absorption of mix (II) which is the mix with a higher value of packing density, and less paste (51 % instead of 92 % in mix I), is considerably less than mix (I). The values obtained for mix (II) and (III) are comparable and in the expected range for UHPFRC materials. Furthermore, for comparison, a concrete often used to build bridge curbs (exposure classes XD3, XF4 after EN 206-1 [22]) has a sorptivity around 300 $g/m^2\sqrt{h}$ (0.061 $lb/ft^2\sqrt{h}$) when it is properly placed and cured [23].

CONCLUSIONS

- With the help of developed packing density model, new UHPFRC mix with reduced EE has been developed.

- In spite of the fact that in the new mixes, 50% of clinker is replaced by limestone filler and 100% of steel fiber is replaced by UHMWPE fibers, the newly developed mixes can yield tensile and compressive strength values comparable to those of steel fiber reinforced UHPC but at the same time having considerably higher tensile strain capacity exceeding 3%.

- After **Table 5**, which is comparing the EE and deadweight of the mixes, 70% reduction in the EE in the new mixes compared to the typical UHPFRC mix as well as reduction of more than 300 kg/m^3 in the dead weight of the material were achieved.

- Considering all the mechanical properties, durability properties and environmental effects, Mix (II) can be an improved version of steel fiber reinforced UHPC which makes the UHPFRC material even more sustainable.

- According to the test results, packing density affects the quality of the matrix and the elastic limit of the cementitious mixes in a way that the mix with higher value of packing density, shows better mechanical properties.

- The durability properties of the cementitious materials have a direct relationship with the packing value of the mix. The higher values of packing density correspond to significantly lower capillary absorption and thus durability in aggressive environements such as exposure classes XD3, XF4.

ACKNOWLEDGMENTS

This project is financially supported by the Swiss National Science Foundation (grant 407040_154063 / 1) through the National Research Program “Energy Turnaround” (NRP 70). The authors would like to acknowledge Dyneema, Omya, LafargeHolcim, and Sika for donating the PE fiber, limestone filler, cement and superplasticizer respectively.

REFERENCES

1. Habert G, Denarié E, Šajna A, Rossi P. Lowering the global warming impact of bridge rehabilitations by using Ultra High Performance Fibre Reinforced Concretes. *Cement and Concrete Composites* 2013,**38**:1-11.
2. Chen J, Chanvillard G. UHPC composites based on glass fibers with high fluidity, ductility, and durability. In: *Ultra-High Performance Concrete and Nanotechnology in Construction. Proceedings of Hipermat*. Kassel; 2012. pp. 265-272.
3. Stengel T, Schießl P. Sustainable construction with UHPC–from life cycle inventory data collection to environmental impact assessment. In: *Proceedings of the 2nd international symposium on ultra high performance concrete. Kassel University Press, Kassel*; 2008. pp. 461-468.
4. Li VC. From micromechanics to structural engineering - the design of cementitious composites for civil engineering applications. *Doboku Gakkai Rombun-Hokokushu/Proceedings of the Japan Society of Civil Engineers* 1993:1-12.
5. Kunieda M, Denarié E, Brühwiler E, Nakamura H. Challenges for strain hardening cementitious composites–deformability versus matrix density. In: *HPFRCC5*; 2007.
6. Kamal A. Material development of UHP-SHCC for repair applications and its evaluation: Nagoya University; 2008.
7. Ranade R, Li VC, Stults MD, Heard WF, Rushing TS. Composite properties of high-strength, high-ductility concrete. *ACI Materials Journal* 2013,**110**:413-422.
8. Curosu I, Liebscher M, Mechtcherine V, Bellmann C, Michel S. Tensile behavior of high-strength strain-hardening cement-based composites (HS-SHCC) made with high-performance polyethylene, aramid and PBO fibers. *Cement and Concrete Research* 2017,**98**:71-81.
9. Powers TC. The properties of fresh concrete. 1969.
10. Fennis S, Walraven J, Den Uijl J. Defined-performance design of ecological concrete. *Materials and structures* 2013,**46**:639-650.

11. de Larrard F. *Concrete mixture proportioning: a scientific approach*: CRC Press; 1999.
12. Sedran T. Rhéologie et rhéométrie des bétons. Application aux bétons autonivelants: Ecole Nationale des Ponts et Chaussées; 1999:220.
13. Fennis S, Walraven J, Den Uijl J. Compaction-interaction packing model: regarding the effect of fillers in concrete mixture design. *Materials and structures* 2013,**46**:463-478.
14. Schwanda F. Das rechnerische Verfahren zur Bestimmung des Hohlraumes und Zementleimanspruches von Zuschlägen und seine Bedeutung für Spannbetonbau. *Zement und Beton* 1966,**37**:13.
15. Denarié E. The generalized CIPM derivation. In. Internal communication: MCS-EPFL 2016.
16. BS812. Testing of aggregates. In: *method of determination of density*. Edited by Institution BS. London: BS; 1995.
17. Marquardt I. *Ein Mischungskonzept für selbstverdichtenden Beton auf der Basis der Volumenkenngrößen und Wasseransprüche der Ausgangsstoffe*; 2001.
18. Denarié E, Sofia L, Brühwiler E. Characterization of the tensile response of strain hardening UHPFRC – Chillon viaducts. In: *AFGC-ACI-fib-RILEM Int. Symposium on Ultra-High Performance Fibre-Reinforced Concrete, UHPFRC 2017*. Montpellier, France; 2017. pp. 241-250.
19. JSCE. Recommendations for Design and Construction of High Performance Fiber Reinforced Cement Composites with Multiple Fine Cracks. In. Tokyo, Japan: Japan Society of Civil Engineers; 2008.
20. SIA, 2052:2016. Béton fibré ultra-performant (BFUP): Matériaux, dimensionnement et exécution Cahier technique SIA 2052. In. fr, Zürich; 2016.
21. EN B. 13057: 2002, Determination of resistance of capillary absorption. *British Standards Institution* 2002,**685**.
22. de Normalisation CE. Concrete. Part 1: Specification, performance, production and conformity. *EN206-1, CEN* 2000,**69**.
23. Denarié E, Brühwiler E. Cast-on site UHPFRC for improvement of existing structures–achievements over the last 10 years in practice and research. In: *7th workshop on High Performance Fiber Reinforced Cement Composites, 1-3, June 2015, Stuttgart, Germany*; 2015.
24. LMC. Absorption d'eau par capillarité. In. LMC report 298/14: EPFL; 2015.

TABLES AND FIGURES

Table 1– *K* values for various packing processes [11]

Packing process		*K* value
dry	Pouring	4.1
	Sticking with a rod	4.5
	Vibration	4.75
	Vibration + compression 10 kPa	9
wet	Smooth thick paste	6.7
	Proctor test	12
virtual	-	∞

Table 2–Mix design and corresponding packing density of the mixes

Component *kg/m³/(lb/ft³)*	Mix I	Mix II	Mix III
Cement	720.8 (45.00)	547.5 (34.18)	
Silica fume	252.3 (15.75)	191.6 (11.96)	
Betocarb-SL	241.0 (15.05)	183.1 (11.43)	
Betoflow-D	551.8 (34.45)	419.1 (26.16)	Premix
Fine Sand	0	616.4 (38.48)	(confidential)
W/B	0.145	0.145	
Water	225.5 (14.08)	178.2 (11.12)	
HRWRA	18.2 (1.14)	28.7 (1.79)	
$Ca(NO_3)_2$	0.05 (0.003)	0.03 (0.002)	
UHMW PE fiber (Dyneema® SK99)	19.6 (1.22)	19.6 (1.22)	0
Steel fiber (14/0.2)	0	0	240 (15)

Packing density	0.787	0.845	~ 0.89 (estimated)

Table 3–Compressive strength of the mixes at 28 days

Mix code	Compressive strength [MPa]/(ksi)
Mix I	81.1 (11.8)
Mix II	115.4 (16.7)
Mix III	113.8 (16.5)

Table 4– Water absorption coefficient in gr/m^2√h (lb/ft^3√h) at 28 days [24]

Mix code	Upper face	Lower face
Mix I	200 (0.041)	141 (0.029)
Mix II	51 (0.010)	49 (0.010)
Mix III	23 (0.005)	
Concrete	300 (0.061)	

Table 5–Comparison of EE and specific weight between the mixes

		Mix (III)	Mix (I)	Mix (II)
Total EE	[MJ/m^3] (therm/ft^3)	~ 20'000 (5.4)*	6'670 (1.8)	6'400 (1.7)
Specific weight	[kg/m^3] (lb/ft^3)	~ 2'500 (156)*	2'030 (127)	2'185 (136)

*: estimated

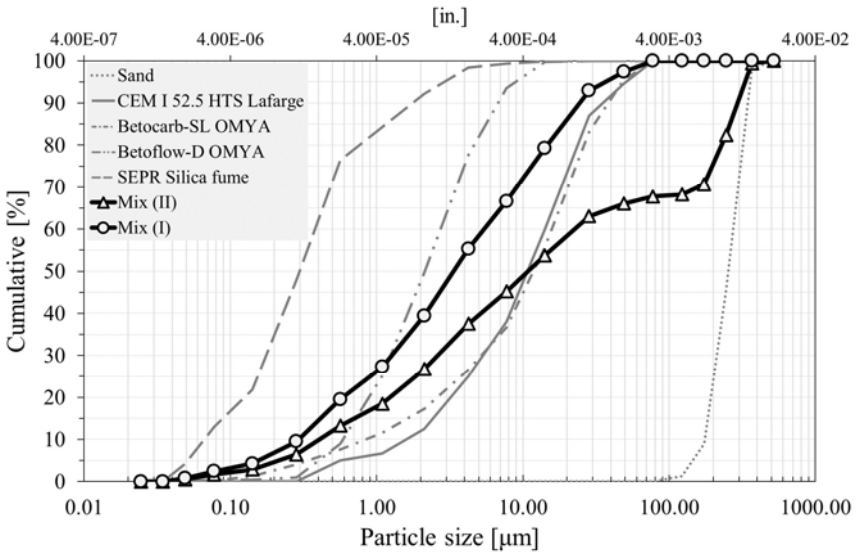

Fig. 1 –PSD curves of the components

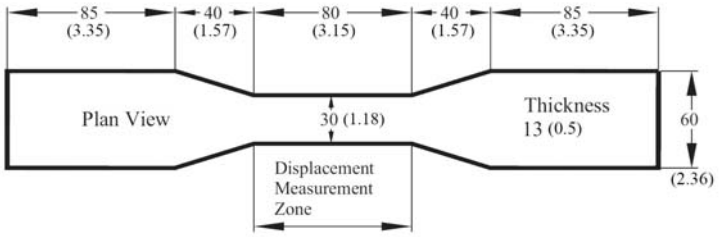

Fig. 2 –Dimensions of direct tensile specimen in mm (inches)

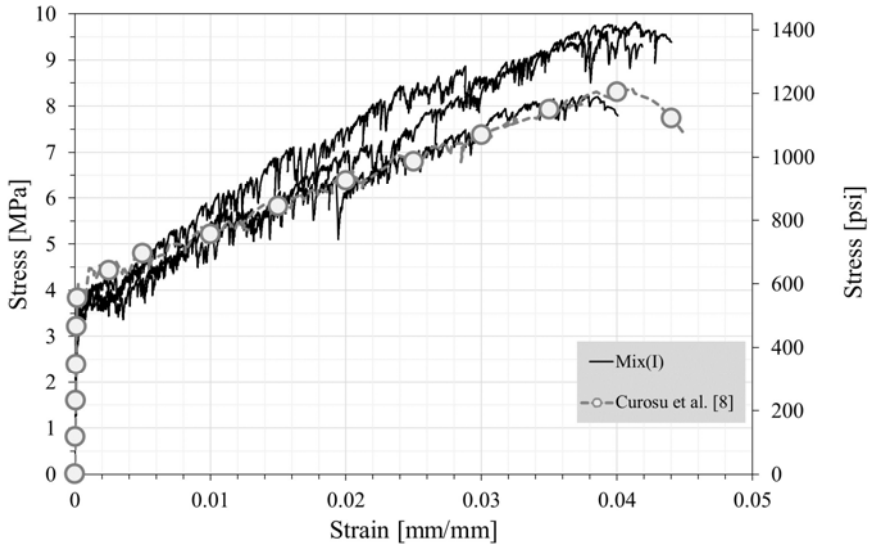

Fig. 3 –Tensile response of Mix (I)

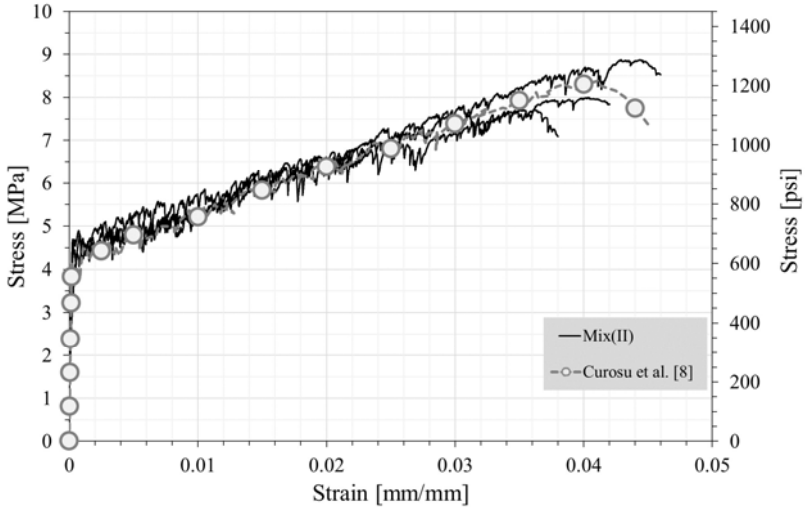

Fig. 4 –Tensile response of Mix (II)

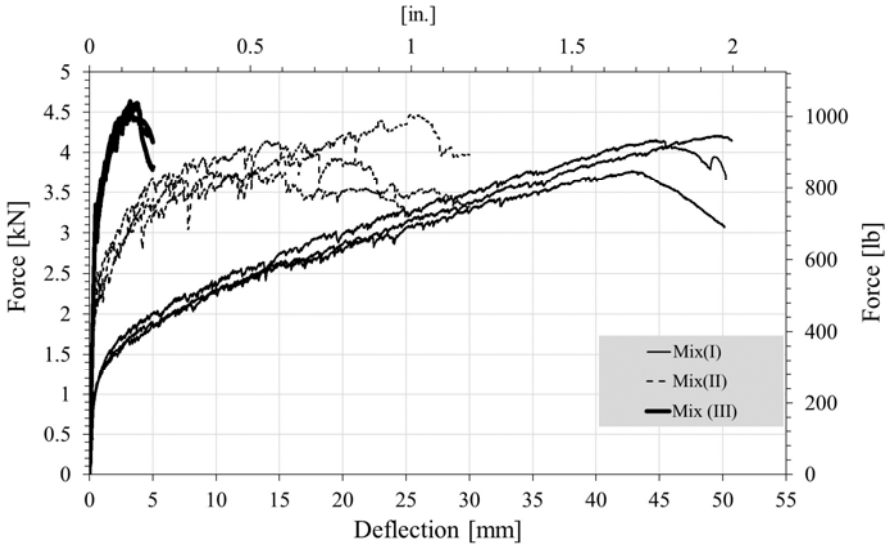

Fig. 5 –4-point bending behavior of the mixes

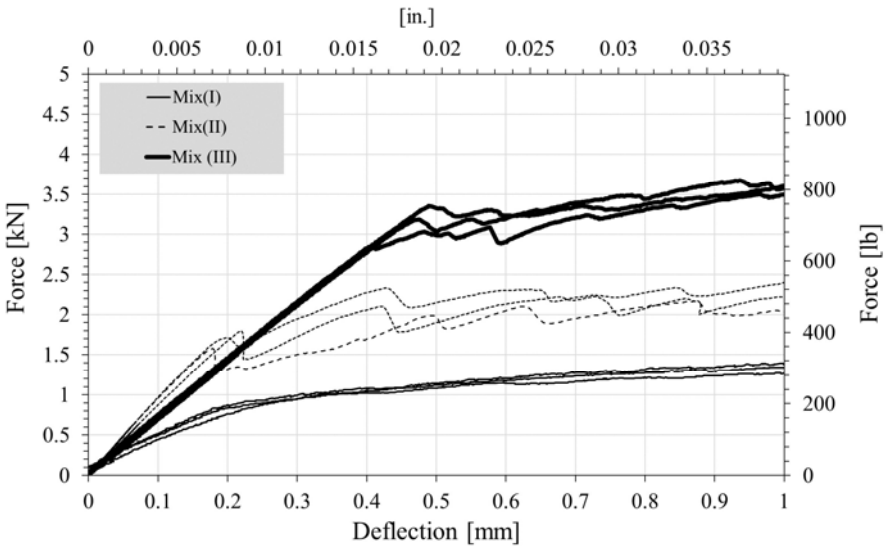

Fig. 6 –Zoom in on the linear part of 4-point bending behavior of the mixes